

## Load Distribution Factors of Simply Supported Concrete T-beam Bridges under Typical Freight Vehicle Loads

Junyuan Yan<sup>1</sup>, Lulu Liu<sup>1,\*</sup> and Ningyuan Shi<sup>2</sup>

<sup>1</sup>College of Engineering and Architecture, Qingdao Agricultural University, Qingdao 266109, China

<sup>2</sup>Sauder School of Business, The University of British Columbia, Vancouver V6T 1Z2, Canada

Received 16 December 2023; Accepted 1 March 2024

### Abstract

Accurate evaluation of load distribution behavior is crucial to the safety evaluation and normal operation of short- and medium-span concrete girder bridges. In this study, 3D finite element analysis was performed to calculate the load distribution factors (LDFs) for a sample of reinforced concrete T-beam bridges under representative typical freight vehicles and the results were compared with those obtained by the American Association of State Highway and Transportation Officials (AASHTO) specification. The parameters that influenced the LDF, namely, transverse loading position, bridge span length, and vehicle type, were analyzed. Results demonstrate that the transverse loading position has a considerable influence on the LDF. The LDF of the interior girder decreases by 45% when the vehicle moves from the centerline of the bridge to the side of the barrier. For the 20 m T-beam bridge, the LDFs of the interior and exterior girders reach the maximum value in the allowable range of the vehicle transverse position, and with the increase in span length, LDF decreases gradually. Among all the loading vehicles, the three-axle truck has the largest LDF, which decreases with the increase in the number of axles. Compared with the LDF in the AASHTO specification, the LDF obtained by finite element analysis is reduced by 24.5%–40.3%, and this reduction can effectively improve the load rating level of bridges in service. The proposed method provides a valuable reference for the safety assessment of bridges in service, which can effectively avoid unnecessary maintenance and reconstruction of old bridges.

*Keywords:* Load distribution factor, typical freight vehicle, T-beam bridge, finite element analysis

### 1. Introduction

In the past few decades, China has experienced a period of large-scale bridge construction. Chinese bridges have gradually entered the post-construction market era, and most of the bridges built at the early stage are subjected to problems, such as low design load level and insufficient safety redundancy [1]. Therefore, accurate evaluation of bridge capacity has become an important topic in bridge operation and management. In multi-girder bridges, the girders, as the primary load carrying members, need to resist the live load. Therefore, the load distribution factor (LDF) must be accurately calculated for the safe operation of newly designed and existing bridges [2–5]. If the live load distributed to a girder is not accurately evaluated, the bridge may be damaged or even crushed before it reaches the end of its designed service life [6].

In existing studies, most of the loading vehicles used in the calculation of LDF are designed trucks. With the development of the automobile industry and social economy, actual traffic loads have changed considerably compared with the loads investigated during the establishment of previous specifications [7]. LDF has changed compared with that specified in bridge design codes because of the diversity of vehicle type and changes in vehicle weight and transverse position. Accurate and comprehensive traffic loads can now be obtained because of the improvement of vehicle information collection technology. Calculating the LDFs of existing bridges in accordance with the measured vehicle

type, gross weight, and transverse position is important for accurately evaluating the load-carrying capacity of existing bridges.

With reference to the traffic load survey in the *Study of Highway Bridge Vehicle Loads* [8] conducted at multiple measuring sites in the Chinese territory, typical freight vehicles that could represent actual vehicle loads are selected in the current study, and the LDFs of short- and medium-span reinforced concrete T-beam bridges are calculated using 3D finite element analysis. The effects of bridge span length, vehicle type, and transverse loading position on the LDFs are examined, and the results are compared with those determined based on the American Association of State Highway and Transportation Officials (AASHTO) specification [9].

### 2. State of the art

At present, the methods used to determine LDF mainly include the equations in bridge design code, field test, and finite element analysis. In general, field test is conducted to validate the accuracy of finite element analysis [10–12]. Kidd et al. [6] analyzed the LDFs of double tee girder bridges through field testing and compared them with those specified in the AASHTO code. The results showed that the LDF specified in the AASHTO code is conservative. Kong et al. [13] analyzed the moment distribution factors of composite bridges with multi-box girders by using the rigid-jointed girder method and proposed an improved formula to compute LDF. Zhao et al. [14] calculated the LDFs of

\*E-mail address: liululu\_2010@163.com

ISSN: 1791-2377 © 2024 School of Science, DUTH. All rights reserved.

doi:10.25103/jestr.172.06

hollow slab bridges by finite element analysis and considered the effects of span length, skew, and bridge deck thickness. The AASHTO specification is found to be conservative compared with finite element analysis, and this conservatism decreases as the skew and span length of hollow-slab bridges increase. Torres et al. [15] analyzed the effects of bridge span length, girder spacing, skew, and deck thickness on LDF and found poor agreement between finite element analysis and AASHTO equations. Using bridge construction parameters in practical engineering, Razzaq et al. [16] studied the LDFs of composite girder bridges under vehicle loads through the finite element analysis method. A set of empirical expressions to calculate the LDFs of exterior and interior girders were developed considering the stiffness and spacing of girders, span length, and number of girders. Ravazdezh et al. [17] found that compared with the 3D finite element analysis method, the 2D methodology with LDF may overestimate the member bending moment and shear force, resulting in an underestimation of the bridge rating factor. This phenomenon may be due to the oversimplification of bridge components and some nonstructural components, such as barriers, sidewalks, and diaphragms. The above mentioned studies only consider the effects of the structural features of bridges on the load distribution behavior, and in some cases, the bridge models are oversimplified to achieve calculation efficiency, and this may have affected the accuracy of the calculation results.

When analyzing the LDFs of multi-girder bridges, previous researchers mainly consider the structural factors of bridges and often ignore the influence of vehicle type and transverse loading position on LDFs. Yanik and Higgins [7] proposed an LDF calculation method based on three different average daily traffic volumes by using probability and statistical methods in accordance with actual collected weigh-in-motion data. The results showed that the accuracy of weigh-in-motion data considerably influences the calculation results, but only the effect of average daily traffic volume on LDF is considered in the study. Seo and Hu [12] studied the LDFs of girder bridges under the load of agricultural vehicles and considered the effects of vehicle weight, axle weight, wheelbase, vehicle width, however, the vehicle type is limited to agricultural vehicles. Ndong et al. [3] investigated the LDFs of steel girder bridges under the action of freight and emergency vehicles via finite element analysis. The results showed that vehicle type remarkably affects LDF, but the transverse position of vehicles is not fully considered by the researcher.

The main parameters that affect LDF accepted by most researchers are girder spacing, bridge span length, longitudinal stiffness, deck thickness, and vehicle type. The effects of vehicle type and transverse loading position on LDF have been rarely explored. In addition, to improve the calculation efficiency of LDF, researchers simplify the bridge model into a 2D component, which may affect the accuracy of the calculation results. To address the deficiencies of existing studies, the current research constructs 3D models of five simply supported reinforced concrete T-beam bridges with different span lengths, and freight vehicles at multiple measuring sites in the Chinese territory are adopted as the loading vehicles. The transverse position of the vehicles is considered. Then, LDFs under the loading action of typical freight vehicles are investigated via finite element analysis, and the results are compared with the values specified in the AASHTO code.

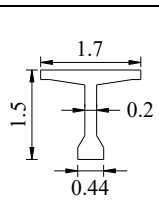
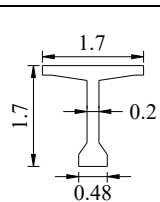
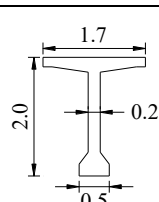
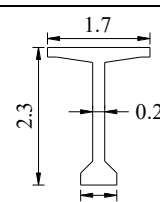
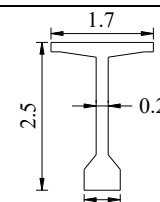
The remainder of this study is organized as follows. In Section 3, the parameters of typical freight vehicles and the finite element analysis method for LDF are introduced. In Section 4, the effects of transverse loading position, bridge span length, and vehicle type on LDF are analyzed, and the finite element analysis results are compared with the values specified in the AASHTO code. In Section 5, the analysis results are summarized, and the limitations of this study are given.

### 3. Methodology

#### 3.1 Selected bridges

Short- and medium-span highway bridges account for a large proportion in China's bridge construction in terms of quantity and length [18]. Concrete T-beam bridges are the common structural form in short- and medium-span girder bridges. Therefore, simply supported concrete T-beam bridges were selected as the study objects in this research, and their LDFs under the loading action of typical freight vehicles were analyzed. The span lengths of the selected T-beam bridges are 20, 25, 30, 35, and 40 m, and the corresponding girder heights are 1.5, 1.7, 2.0, 2.3, and 2.5 m. The web thickness is 0.2 m, the top flange width of the interior girder is 1.7 m, and the top flange width of the exterior girder is 2.05 m. The dimensions of the interior girders of the bridges with different span lengths are shown in Table 1.

**Table 1.** Interior girder dimensions of the T-beam bridges

| Span length/m | 20  | 25  | 30  | 35  | 40  |
|---------------|---|---|---|---|---|
| Dimensions/m  |  |  |  |  |  |

The typical cross section of a 20 m T-beam bridge is shown in Fig. 1. The bridge consists of five girders with a spacing of 2.4 m. The total bridge deck width is 12 m, the width of the barriers is 0.5 m, and the clear width of the bridge deck is 11 m. The adjacent girders are connected through cast-in-place concrete with a joint width of 0.7 m. This connection mode can be approximately regarded as a

rigid connection, and it is modeled by coupling the nodes at the same location in the finite element model.

#### 3.2 Loading vehicles

At present, many kinds of vehicles operate in China's highway system, and they differ remarkably in terms of vehicle weight and geometrical parameters. In this study, the

typical freight vehicles given in the *Study of Highway Bridge Vehicle Loads* [8] are selected as the loading vehicles and the proportional distribution of vehicle type is shown in Fig. 2. The figure indicates that the freight vehicles at the majority of the measuring sites in China are dominated by two- and six-axle trucks, six-axle trucks account for a large proportion (53.3%), and two-axle trucks account for 20.9%. The proportions of three-, four-, and five-axle trucks are 9.3%, 10.4%, and 5.8%, respectively, and that of vehicles with more than six axles is 0.3%.

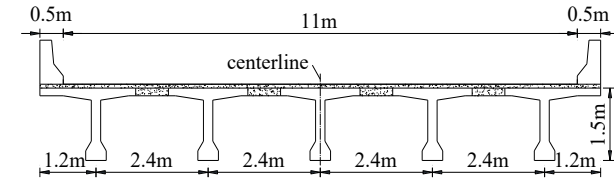


Fig. 1. Cross section of a 20 m T-beam bridge

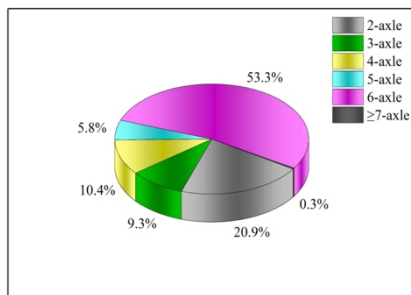


Fig. 2. Proportions of freight vehicles

The characteristics and average gross vehicle weight of each truck are shown in Table 2. The axle configuration and axle load distribution ratio of the vehicles are given in Table

2, and the gross vehicle weight is distributed to each axle in accordance with the axle load ratio shown in the table. The wheelbase of vehicles in Table 2 was determined using the wheelbase information of trucks sold in the market in combination with weigh-in-motion data [8], which are representative. In the finite element analysis, the axle was modeled by concentrated load, which was evenly distributed to the left and right wheels, as shown in Fig. 3.

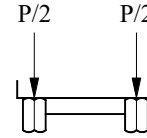


Fig. 3. Lateral distribution of axle weight

### 3.3 Finite element analysis

In this study, the LDFs of T-beam bridges were calculated through finite element analysis, and finite element models of the bridges were constructed with ANSYS 2022. The concrete bridge components, including the girders, diaphragms, and barriers, are modeled using SOLID45 elements. These elements have three translational degrees of freedom with sizes of 0.2 m (length) × 0.1 m (width) × 0.1 m (height), and the bridge deck pavement is simulated using PLANE42 elements. Full composite action is assumed between the girders and the bridge deck pavement, so the contact surface between the girders and the bridge deck pavement in the finite element model is simulated using the same nodes at the interface. The bridge girders is simply supported with a roller at one end and a hinge at the other end.

Table 2. Characteristics and average gross vehicle weight of the trucks

| Vehicle type     | Vehicle sketch | Average gross vehicle weight /t |
|------------------|----------------|---------------------------------|
| Two-axle truck   |                | 18.36                           |
| Three-axle truck |                | 34.87                           |
| Four-axle truck  |                | 45.74                           |
| Five-axle truck  |                | 54.26                           |
| Six-axle truck   |                | 63.12                           |

The lateral loading range of the freight vehicles is shown in Fig. 4. The loading vehicle moves from the centerline of

the bridge to the side of the barrier. In consideration of the safe distance between the wheels and the barrier, the loading

is stopped when the distance between the outer wheels and the edge of the barrier is 0.6 m. Within the allowable loading range shown in Fig. 4, the vehicle moves laterally by a step of 0.2 m, and a total of 21 loading cases are generated.

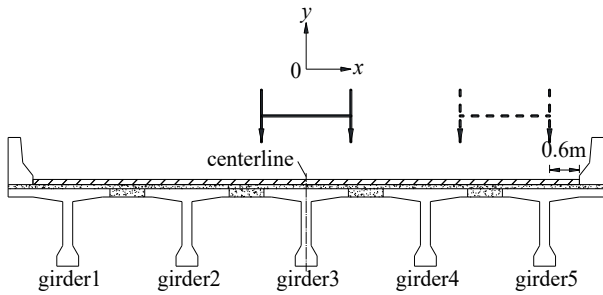


Fig. 4. Allowable lateral loading range of the vehicles

The moment LDFs for different girders are defined as the ratio of the bending moment at the mid-span of a particular girder to the sum of the bending moments at the mid-span of all girders. Finite element analysis was conducted under different loading conditions. The bending moment,  $M_i$ , of each girder at the mid-span was obtained, and the LDF of girder  $i$  was determined using the formula:

$$LDF = \frac{M_i}{\sum M_i} \quad (1)$$

where LDF represents the load distribution factor of each girder and  $M_i$  denotes the bending moment of girder  $i$  at the mid-span.

#### 4. Result Analysis and Discussion

##### 4.1 Effect of transverse loading position

A simply supported T-beam bridge with a span length of 20 m was adopted as an example, and the changes in the LDFs of each girder with the transverse loading position under the loading action of a two-axle truck are displayed in Fig. 5. When the vehicle is near the centerline of the bridge, girder 3 has the largest LDF among the girders, and it undertakes the largest live load. When the vehicle moves away from the centerline of the bridge, the live load carried by girder 3 decreases, and the live load distributed to girder 4 and 5 increases. When the distance between the loading vehicle and the barrier is reduced to a safe distance, the LDF of girder 5 reaches the maximum. Girder 1 and 2 share minimal live load because they are far from the loading position. On the basis of the symmetry of the structure, analysis is performed only in the right side of the centerline of the bridge, so the LDFs of girder 3, girder 4, and girder 5 are analyzed next.

##### 4.2 Effect of bridge span length

With a two-axle truck as the loading vehicle, the LDFs of the T-beam bridges with different span lengths in the lateral loading range of the vehicles were analyzed. As indicated in Fig. 6(a), among the girders, girder 3 with a span length of 20 m has the largest LDF. As the loading vehicle moves, the LDF of the T-beam bridge with a span length of 35 m gradually exceeds that of the T-beam bridge with a span length of 20 m. Moreover, the LDF of the 20 m T-beam bridge is comparatively more sensitive to the changes in the

transverse loading position. As the loading vehicle moves from the centerline of the bridge to the side of the barrier, the LDF of girder 3 decreases from 0.286 to 0.158, indicating a decrease of 45%. When the span length is 35 m, the transverse loading position of the vehicles has relatively small influence on the LDF of girder 3, and the LDF decreases by 37% when the vehicle moves from the centerline of the bridge to the side of the barrier.

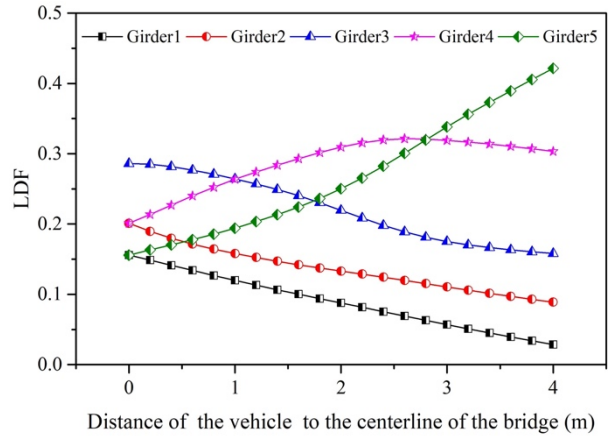
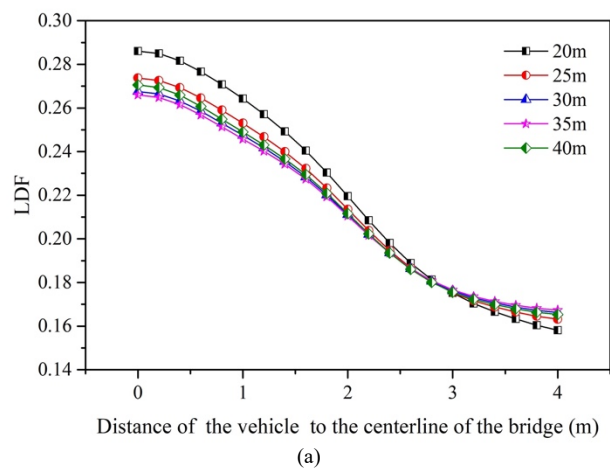


Fig. 5. Changes in the LDFs of each girder with the transverse loading position (span = 20 m)

Fig. 6(b) shows the LDF of girder 4. When the vehicle moves within the allowable transverse loading range, the T-beam bridge with a span length of 20 m has the largest LDF among the T-beam bridges with various span lengths, and no substantial differences are observed among the T-beam bridges with other span lengths in terms of LDFs. When the vehicle moves to the side of the barrier, LDF is influenced only slightly by span length, and the LDFs of the T-beam bridges with various span lengths are approximate. Fig. 6(c) presents the LDF of girder 5. When the loading vehicle is near the centerline of the bridge, the LDF of the T-beam bridge with a span length of 20 m has the minimum value. As the vehicle moves near the barrier, the LDF of the T-beam bridge with a span length of 20 m reaches the maximum value and exceeds that of the bridges with other span lengths.



(a)

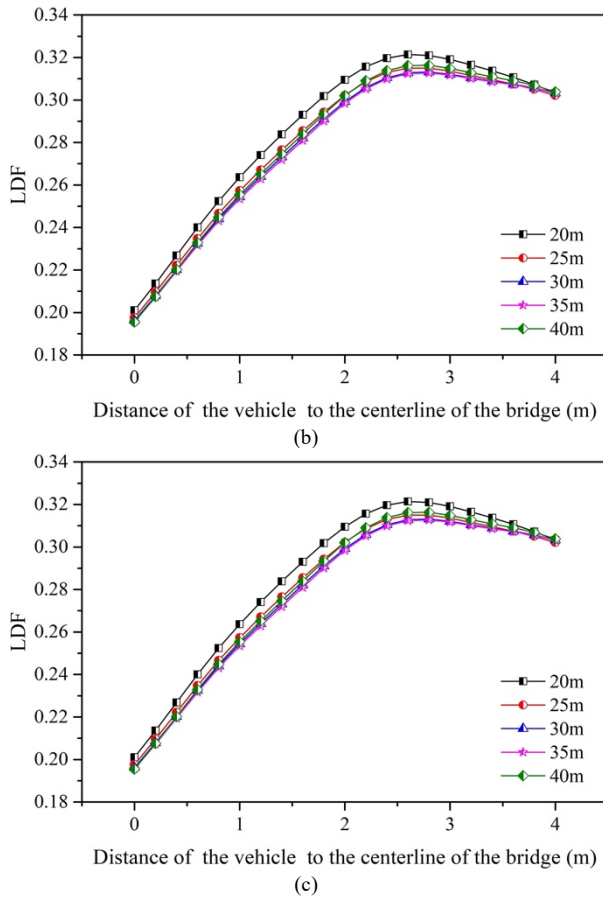


Fig. 6. LDFs of T-beam bridges with different span lengths: (a) Girder 3, (b) Girder 4, (c) Girder 5

4.3 Effect of vehicle type

Taking a T-beam bridge with a span length of 40 m as an example, the influence of vehicle type on the LDF was analyzed, and the calculation results are shown in Fig. 7. The LDFs of the two- and three-axle trucks are close possibly because the wheelbase of the first two axles of the three-axle truck is similar to that of the two-axle truck.

As illustrated in Fig. 7(a), when the vehicle is loaded in the center of the bridge, the differences in the LDFs of the various vehicle types are large. As the loading vehicle moves toward the side of the barrier, the LDF difference between the girders decreases initially and then increases. Fig. 7(b) indicates that when the loading vehicle is near the centerline of the bridge, vehicle type nearly has no effect on the LDF of girder 4. As the vehicle moves toward the barrier, the LDF difference induced by vehicle type firstly increases and then decreases. As shown in Fig. 7(c), the LDF of the exterior girder (girder 5) is influenced slightly by the change in vehicle type. When the vehicle moves to the side of the barrier, the LDFs under the loading action of different vehicle types are nearly identical.

4.4 Comparison with the AASHTO specification

The AASHTO code specifies the calculation method for the LDF of concrete T-beam bridges. The LDF of the exterior girder can be calculated with the lever method, and the LDF of the interior girder can be solved through the following formula:

$$DF_{M,int} = 0.06 + \left(\frac{S}{14}\right)^{0.4} \left(\frac{S}{L}\right)^{0.3} \left(\frac{K_g}{12.0Lt_s^3}\right)^{0.1} \quad (2)$$

where  $S$  represents girder spacing,  $L$  is the bridge span length,  $t_s$  denotes the thickness of the deck, and  $K_g$  is the longitudinal stiffness of the bridge.

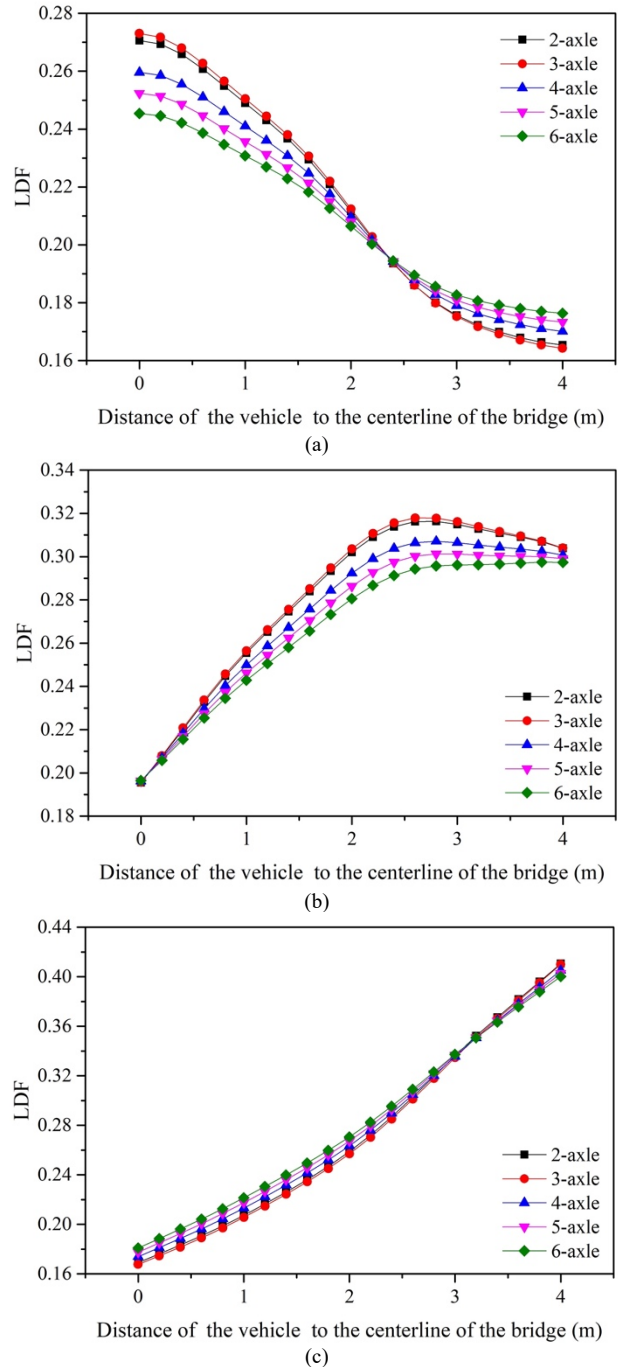


Fig. 7. Load distribution factors: (a) Girder 3, (b) Girder 4, (c) Girder 5

The difference between the LDF obtained by finite element analysis and the LDF specified in the AASHTO code is determined. A parameter that represents the relative difference between the two is defined as RD, and its calculation formula is as follows:

$$RD = \frac{LDF_{AASHTO} - LDF_{FEA}}{LDF_{AASHTO}} \times 100\% \quad (3)$$

where  $LDF_{AASHTO}$  is the LDF specified in the AASHTO code, and  $LDF_{FEA}$  denotes the maximum LDF acquired through finite element analysis.

**Table 3.** Comparison of analytical and specified LDFs for concrete T-beam bridges

| (a) Interior girder |                        |       |       |       |       |
|---------------------|------------------------|-------|-------|-------|-------|
| LDF                 | Bridge span length (m) |       |       |       |       |
|                     | 20                     | 25    | 30    | 35    | 40    |
| AASHTO              | 0.502                  | 0.473 | 0.451 | 0.433 | 0.419 |
| FEM                 | 0.321                  | 0.315 | 0.313 | 0.313 | 0.316 |
| RD                  | 36.0%                  | 33.4% | 30.6% | 27.8% | 24.5% |
| (b) Exterior girder |                        |       |       |       |       |
| LDF                 | Bridge span length (m) |       |       |       |       |
|                     | 20                     | 25    | 30    | 35    | 40    |
| AASHTO              | 0.685                  | 0.685 | 0.685 | 0.685 | 0.685 |
| FEM                 | 0.411                  | 0.409 | 0.411 | 0.413 | 0.423 |
| RD                  | 40.0%                  | 40.3% | 40.0% | 39.7% | 38.2% |

Table. 3 shows the comparison of the finite element analysis results and those of the AASHTO specification. The calculation results of AASHTO code for the interior and exterior girders are conservative. For the interior girders, the smaller the span length is, the greater the relative difference is. The relative difference reaches 36.0% at the span length of 20 m. For the exterior girders, the relative difference decreases with the increase in span length, but the change is small. The relative difference in the LDFs of the interior girders is more sensitive to the change in span length compared with the relative difference in the LDFs of the exterior girders.

## 5. Conclusion

To accurately evaluate the LDFs of short- and medium-span concrete T-beam bridges, 3D models of five simply supported concrete T-beam bridges with different span lengths were constructed, and five representative freight vehicles were selected as loading vehicles. The effects of

transverse loading position, bridge span length, and vehicle type on the LDFs were analyzed with the finite element method, and the LDFs were compared with those provided in the AASHTO code. The following conclusions were drawn.

(1) The changes in the vehicle transverse loading position considerably affects the LDF. As the loading vehicle moves from the centerline of the bridge to the side of the barrier, the LDF of the interior girder decreases, while that of the exterior girder increases and the exterior girder becomes the critical girder instead of the interior girder.

(2) The type of the loading vehicle exerts a considerable influence on the LDF of the interior girder, but it has only a minimal influence on the LDF of the exterior girder. For the interior girder, the larger the number of axles is, the smaller the LDF is.

(3) Compared with the LDFs obtained by finite element analysis, the LDFs specified in the AASHTO code are conservative. The latter may lead to a low bridge rating factor and unnecessary maintenance or reconstruction.

In this study, the damage or aging of existing components is not considered in the finite element analysis. During the evaluation of the safety of existing bridges in practical engineering, the finite element model should be updated in accordance with actual bridge detection and load testing results to realize a targeted analysis of specific problems and maximize the accuracy of finite element analysis.

## Acknowledgements

The authors are grateful for the support provided by the Scientific Research Fund of Qingdao Agricultural University (Grant No. 663/1120049).

This is an Open Access article distributed under the terms of the Creative Commons Attribution License.



## References

- [1] Edit. Dept. of China J. Highw. Transp., "Review on China's bridges engineering research: 2021," (in Chinese), *China J. Highw. Transp.*, vol. 34, no. 2, pp.1-97, Feb. 2021, doi: 10.19721/j.cnki.1001-7372.2021.02.001.
- [2] W. Choi, I. Mohseni, J. Park, and J. Kang, "Development of live load distribution factor equation for concrete multicell box-girder bridges under vehicle loading," *Int. J. Concr. Struct. Mater.*, vol. 13, no. 1, Mar., 2019, Art. no. 22, doi: 10.1186/s40069-019-0336-1.
- [3] A. K. Ndong, M. M. Sherif, B. Kassner, O. E. Ozbulut, and D. K. Harris, "Refined analysis of steel girder bridges for computation of live load distribution factors considering effects of freight and emergency vehicles," *Eng. Struct.*, vol.293, Jul., 2023, Art. no. 116630, doi: 10.1016/j.engstruct.2023.116630.
- [4] J. Yan, L. Deng, and W. He, "Evaluation of existing prestressed concrete bridges considering the randomness of live load distribution factor due to random vehicle loading position," *Adv. Struct. Eng.*, vol. 20, no. 5, pp. 737-746, May, 2017, doi: 10.1177/1369433216664350.
- [5] S. W. Kim, D. W. Yun, D. U. Park, S. J. Chang, and J. B. Park, "Estimation of live load distribution factor for a PSC I girder bridge in an ambient vibration test," *Appl. Sci-Basel*, vol. 11, no. 22, Nov., 2021, Art. no. 11010, doi: 10.3390/app112211010.
- [6] B. Kidd, S. Rimal, J. Seo, M. Tazarv, and N. Wehbe, "Field distribution factors and dynamic load allowance for simply supported double-tee girder bridges," *Struct. Eng. Mech.*, vol. 82, no. 1, pp. 69-79, Apr., 2022, doi: 10.12989/sem.2022.82.1.069.
- [7] A. Yanik and C. Higgins, "Weigh-in-Motion load effects and statistical approaches for development of live load factors," *Struct. Eng. Mech.*, vol. 76, no. 1, pp. 1-15, Oct., 2020, doi: 10.12989/sem.2020.76.1.001.
- [8] X. G. Zhang, "Study and adaptability analysis of highway bridge vehicle loads" in *Study of Highway Bridge Vehicle Loads*. Beijing, China: CC Press, (in Chinese), 2014, ch. 4, pp. 90-95.
- [9] *AASHTO LRFD Bridge Design Specifications*, AASHTO LRFDDBS-9, AASHTO, Washington, DC, USA, 2020.
- [10] Z. Yousif and R. Hindi, "AASHTO-LRFD live load distribution for beam-and-slab bridges: limitations and applicability," *J. Bridge Eng.*, vol. 12, no. 6, pp. 765-773, Nov., 2007.
- [11] M. Maguire, C. D. Moen; C. Roberts-Wollmann, and T. Cousins, "Field verification of simplified analysis procedures for segmental concrete bridges," *J. Struct. Eng.*, vol. 141, no. 1, Jan., 2015, Art. no. D4014007, doi: 10.1061/(ASCE)ST.1943-541X.0001111.
- [12] J. Seo and J. W. Hu, "Influence of atypical vehicle types on girder distribution factors of secondary road steel-concrete composite bridges," *J. Perform. Const. Facil.*, vol. 29, no. 2, Apr., 2015, Art. no. 04014064, doi: 10.1061/(ASCE)CF.1943-5509.0000566.
- [13] S. Kong, L. Zhuang, M. Tao, and J. Fan, "Load distribution factor for moment of composite bridges with multi-box girders," *Eng. Struct.*, vol. 215, Jul., 2020, Art. no. 110716, doi: 10.1016/j.engstruct.2020.110716.
- [14] Y. Zhao, X. Cao, Y. Zhou, G. Wang, and R. Tian, "Lateral load distribution for hollow slab bridge: field test investigation," *Int. J. Concr. Struct. Mater.*, vol. 14, no. 1, Apr., 2020, Art. no. 22, doi: 10.1186/s40069-020-0397-1.

- [15] V. Torres, N. Zolghadri, M. Maguire, P. Barr, and M. Halling, "Experimental and analytical investigation of live-load distribution factors for double tee bridges," *J. Perform. Const. Facil.*, vol. 33, no. 1, Feb, 2019, Art. no. 04018107, doi: 10.1061/(ASCE)CF.1943-5509.0001259.
- [16] M. K. Razzaq, K. Sennah, and F. Ghrib, "Live load distribution factors for simply-supported composite steel I-girder bridges," *J. Constr. Steel. Res.*, vol. 181, Mar., 2021, Art. no. 106612, doi: 10.1016/j.jcsr.2021.106612.
- [17] F. Ravazdezh, S. Seok, G. Haikal, and J. A. Ramirez, "Effect of nonstructural elements on lateral load distribution and rating of slab and T-beam bridges," *J. Bridge Eng.*, vol. 26, no. 9, Sep., 2021, Art. no. 040221063, doi: 10.1061/(ASCE)BE.1943-5592.0001766.
- [18] S. H. Li, R. F. Nie, and R. N. Jiang, "Truck weight limits of RC beam bridges based on the flexural and shear capacities," (in Chinese), *Chin. Civil Eng. J.*, vol. 51, no. 2, pp.74-80, Feb., 2018, doi: 10.15951/j.tmgcxb.2018.02.008.